Int J Adv Manuf Technol (2006) 31: 258–267
DOI 10.1007/s00170-005-0197-4

ORIGINAL ARTICLE

V. K. Gorana · V. K. Jain · G. K. Lal

Prediction of surface roughness during abrasive flow machining

Received: 19 June 2004 / Accepted: 10 June 2005 / Published online: 24 May 2006

Abstract An analytical model is proposed to simulate and predict the surface roughness for different machining conditions in abrasive flow machining (AFM). The kinematic analysis is used to model the interaction between grain and workpiece. Fundamental AFM parameters, such as the grain size, grain concentration, active grain density, grain spacing, forces on the grain, initial topography, and initial surface finish (R_a value) of the workpiece are used to describe the grain-workpiece interaction. The AFM process is studied under a systematic variation of grain size, grain concentration and extrusion pressure with initial surface finish of the workpiece. Simulation results show that the proposed model gives results that are consistent with experimental results.

Keywords Active grain density · Forces on a grain · Grain spacing · Initial surface finish · Initial topography

Abbreviations A: Projected area of contact between the workpiece and abrasive grain, mm^2 · A_1: Area of the cylindrical workpiece in contact with the medium, mm^2 · A_2: Area of cuboidal element from any section of medium, mm^2 · A_3, A_4, A_5, A_6, A_7: Areas of peaks and valleys on an assumed surface, mm^2 · $\bar{a}$: Effective grain spacing, mm · b: Diameter of projected area of a grain in contact with the workpiece, mm · $\bar{b}$: Mean diameter of projected area of grain (= mean width of cutting edge), mm · C: Percent abrasive concentration · D: Diameter of a cylindrical workpiece, mm · d_g: Diameter of the abrasive grain, mm · d': Depth of indentation by a grain according to Hertz theory, mm · d'': Depth upto which material is displaced from a triangular peak after one pass, mm · E_m: Modulus of elasticity of workpiece material, N/mm^2 · F_{ng}: Radial force on a single grain during AFM, N · F_{am}: Measured axial force on the cylindrical workpiece during AFM, N · G: Volume ratio of the abrasive grain in medium · G_1: Volume of groove produced by a single grain (Fig. 4), mm^3 · G_2: Volume of side flown material from the groove produced by a single grain (Fig. 4), mm^3 · h_t: Depth of indentation of a cutting tip inside the workpiece, mm · h_{t1}, h_{t2}, h_{t3}, ...h_{tn_s}: Depth of indentation of cutting tips inside the workpiece by grain 1, 2, 3, ...n_s (Fig. 2). · i: Number of pass · L: Sampling length of an assumed surface, mm · l: Length of the cylindrical workpiece, mm · l_t: Base length of the assumed equilateral triangular profile of the workpiece surface, mm · l': Assumed length on the medium surface, mm · l_m: Length of the medium slug passed in one stroke through the workpiece, mm · l_s: Length of stroke in medium cylinder, mm · M_e: Grain mesh number · m: Total number of cutting edges on the l' length of the strip on the medium surface · N: Total number of grains in cuboidal element from any section of the medium (Fig. 3) · P_e: Applied extrusion pressure to medium, MPa · n: Number of grains per unit area · n_1: Number of active grains per unit area on the medium · n_a: Total number of active grains on the whole cylindrical workpiece surface area in contact with the medium · n_s: Average number of grains in one line over the total length of the medium passed in one stroke ($=l_s$) · n_{mv}: Active grain density by multivariable model · p_i: Indenting force acting on ith cutting grain (Fig. 2), N · R: Radius of grain, mm · R_t: Tip radius of the grain (= radius of the grain), mm · R_a: Center line average (CLA) value of surface roughness, μm · $R_{a(new)}$: New CLA value of surface roughness after machining, μm · r_{cy}: Radius of medium cylinder, mm · r_w: Radius of cylindrical workpiece, mm · V: Volume of the cuboidal element, mm^3 · $\bar{w}$: Mean spacing between the grains (or side of a square area assumed to have only one active grain), mm · x, y: Width of the sides of a cuboid (Fig. 3) · σ: Flow stress of workpiece material, N/mm^2

V. K. Gorana · V. K. Jain (✉) · G. K. Lal
Department of Mechanical Engineering,
Indian Institute of Technology,
Kanpur, 208016, India
e-mail: vkjain@iitk.ac.in
Tel.: +91-512-2597916

V. K. Gorana
Department of Mechanical Engineering,
Engineering College,
Kota (Raj.), 324010, India

1 Introduction

Abrasive flow machining (AFM) is a non-traditional finishing process that performs critical deburring and polishing operation by forcing abrasive-laden viscoelastic putty across the workpiece surface [1, 2]. In AFM, two vertically opposed cylinders (Fig. 1) extrude medium back and forth through passages formed between the workpiece and tooling. The process parameters that have a large impact on the AFM performance are the number of cycles, extrusion pressure, grit concentration and size, and fixture design. AFM is employed in aerospace, automotive, semi-conductor, and medical components industries. Because of its inherent characteristics, AFM can be integrated with the overall manufacturing system to replace high cost manual finishing operations [2]. To advance the understanding of complex process it is often necessary to construct a simple model, experimental or mathematical, in which the variables can be changed in an orderly fashion and their effects can be analysed. The model, in general, provides the information, which gives an insight into the nature of phenomenon occurring in the real life situation. In the case of grinding, there have been many attempts in the past to model the surface generated using statistical approaches [3].

Yoshikawa and Sata [4] simulated the grinding process by the Monte Carlo method. Law and Wu [5] developed a grinding model in terms of grains distribution on the abrasive wheel and kinematic grinding conditions. Hamed et al. [6] applied an approach to generate random surfaces by computer simulation which involves the use of a series of ‘unit events’ to produce a surface profile. The work confirmed that the engineering surfaces could be described statistically by a profile having ordinate heights with a Gaussian distribution together with a form of exponential autocorrelation function. Abrahamson et al. [7] showed the effect of initial surface finish on the wear of sliding surfaces. Jain and Jain [8] analyzed and simulated the profile of the finished surface by the interaction of abrasive grains with the workpiece in abrasive flow machining process. Pandey et al. [9] proposed the equation to estimate the center line average value of a parabolic profile. Spurr [10] also gave the equation that estimates the C.L.A. surface roughness value of metals after they have been slid against various grades of abrasive paper and confirmed it experimentally. Dowson and Whomes [11] reported that the inclusion of roughness in the analysis inevitably introduces difficulty in mathematical representation of the surface topography. The surface cannot be described exactly by a simple equation, nor can it be considered entirely random in nature. Any model of the surface will therefore be an approximation. As reported in reference [12], the asperities distributed over a machined surface could generally be assumed to be of conical protuberances. Tsuwa [13] reported a simple concept of probability to find out effective spacing between the cutting edges in the grinding wheel. Jain et al. [14] developed a surface roughness model of the workpiece, which has uniform profile without statistical distribution. They observed that surface roughness value decreases with an increase in piston velocity, piston pressure, percentage concentration of abrasives and grain mesh size for a specified number of cycles. After a certain value of velocity and pressure, surface roughness starts deteriorating due to an increase in depth of indentation.

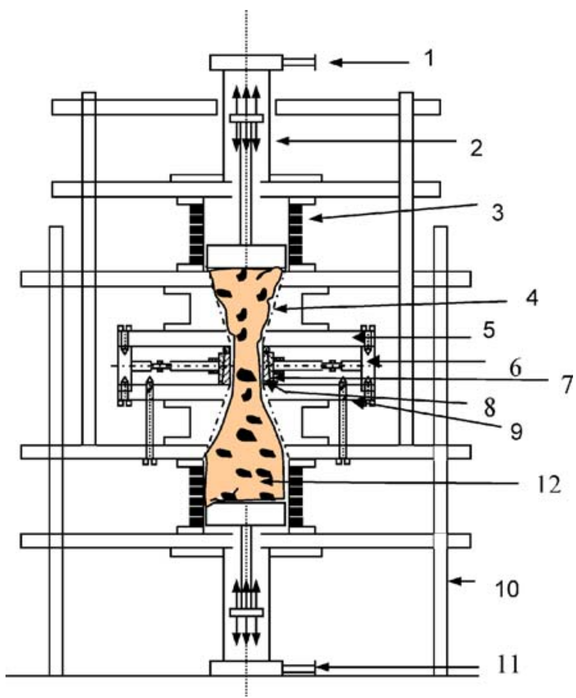

Fig. 1 Schematic diagram of experimental set-up. 1-Hydraulic oil inlet, 2-Hydraulic cylinder, 3-Medium cylinder, 4-Smooth entry profile, 5-Top cover plate, 6-Dynamometer, 7-Central hub, 8-Split cylindrical fixture with workpiece, 9-Bottom cover plate, 10-Support frame, 11-Hydraulic oil outlet, 12-Medium with abrasive particles

The approaches discussed above [7–14], can be applied to model the surface roughness obtained in abrasive flow machining process with certain modifications depending upon the AFM conditions. However, it is assumed that there exists similarity in distribution of abrasive particles in grinding wheel and in medium of AFM. The difference is that in grinding wheel the medium is rigid while in AFM it is flexible having low bonding strength. The study of surface roughness in abrasive flow machining is complicated due to the random nature of the abrasive grain distribution into putty, and very low depth of indentation of abrasive grain and hence minute scale of metal deformation. It is difficult to predict the surface roughness in a deterministic way. However, it can be approximately determined by considering the interaction of a single grain with assumed single equilateral triangular profile of the surface of the workpiece, by mathematical simulation on computer. The surface roughness in AFM is the total outcome due to a large number of grains running in a single row and interacting with the workpiece. By simulating these individual events, it is possible to predict the surface roughness value (R_a). To implement the same, it requires the information about the topography of the AFM medium and the kinematics of the AFM process.

It is concluded [15] that in AFM the mechanics of material removal is rubbing and plowing under the prescribed machining conditions. To draw any conclusion only based on the experimentation may not be enough. Therefore to validate our experimental results, the present paper proposes a simple analytical model, which can predict the surface roughness (R_a value) when interaction between a single spherical abrasive grain and assumed equilateral triangular peaks of the workpiece profile takes place. The analytical model consists of three parts, namely, prediction of (i) active grains density, (ii) forces on a single grain, and (iii) surface roughness value. These responses have been compared with the experimental results. The analytical model enables to predict R_a value of the machined surface in terms of abrasive grain size, normal and axial forces acting on the workpiece, percentage abrasive concentration, properties of the workpiece material, initial R_a value, and passage dimensions of the geometry through which medium flows (diameter and length of the cylindrical workpiece).

2 Prediction of active grain density

In abrasive flow machining, the number of active grains can be estimated analytically in terms of the process parameters. The model of active grains is proposed from the work of Tanka and Ikawa [16] with a few modifications. It is assumed that there exists similarity in distribution of abrasive particles in grinding wheel and abrasive particles in medium used in AFM. The difference is that in grinding wheel the medium is a rigid body while in AFM it is a flexible viscoelastic putty. Following are the assumptions made to simplify the model (Fig. 2).

(1) Fracture and wear of the abrasive grains do not occur and there is no relative displacement between the grains in the medium especially in the finishing zone.
(2) Each of the grains has only one spherical cutting tip and each grain is very small in size, i.e., the number of cutting tips per unit area is equal to the number of grains per unit area on any section of the medium. Tip radius, $R_t = {d_g}/{2}$ (d_g is grain diameter).
(3) In AFM, active grains are in contact with the workpiece under a pressure equal to the flow stress of the workpiece material.
(4) It is assumed that the penetration depth of the cutting tips (h_t) is distributed in the (discrete) steps of h_t in between zero and $\frac{d_g}{2}$ (=R_t) as shown in Fig. 2. The tip height can be estimated [16] as,

$$h_t = \frac{d_g}{2nA_1} \tag{1}$$

where h_t=height of the cutting tip, A_1=area of the internal surface of the cylindrical workpiece, and n=number of grains per unit area.

Let the measured axial force exerted on the workpiece by the grains through the medium be given by F_{am}. When the medium slides over the workpiece surface then at that time F_{am} can be expressed as

$$F_{am} = \sum_{i=1}^{n_a} p_i, \tag{2}$$

where, p_i is the force acting on the ith grain. Total indenting force by the n_a total number of active grains (on the whole cylindrical workpiece surface area in contact with the medium) can also be evaluated theoretically [16] if the flow stress (σ) of the workpiece material is known as,

$$F_{am} = \sum_{i=1}^{n_a} p_i = \frac{1}{2}\,\pi\, R_t\, \sigma\, h_t\, n_a^2 \tag{3}$$

where, R_t is tip radius of the grain (= radius of the grain), and h_t is depth of indentation of the cutting tip inside the workpiece surface.

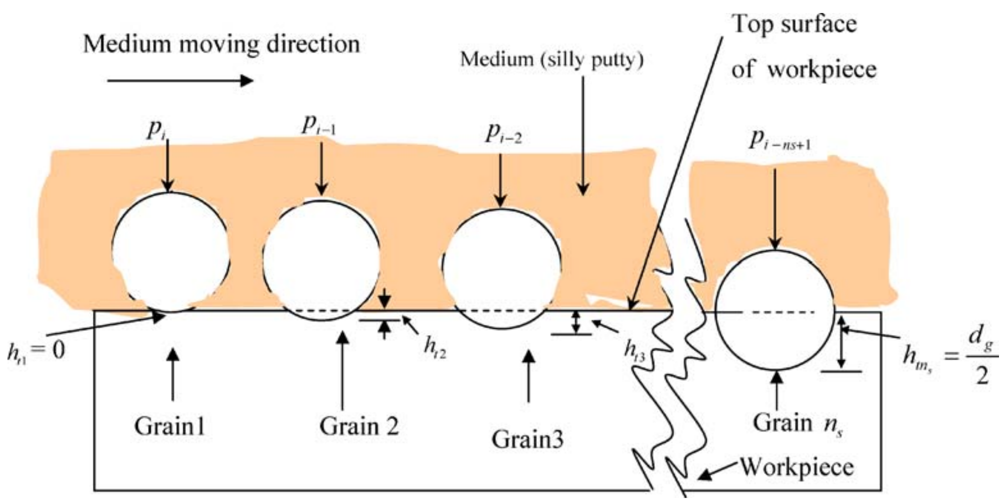

Fig. 2 Model of a part of the medium scratching the workpiece by spherical tips

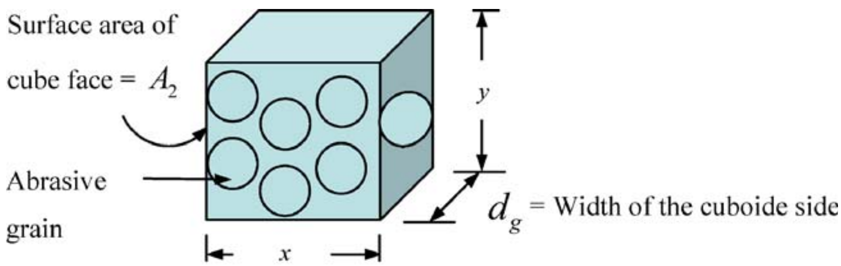

Fig. 3 Element of the medium having side face width equal to d_g

Therefore, using Eq. 3, the number of the active grains in contact with the cylindrical workpiece surface area (over the cylindrical medium slug) is,

$$n_a = \left(\frac{2 \times F_{am}}{\pi\ \sigma\ R_t\ h_t}\right)^{\frac{1}{2}}. \tag{4}$$

Since it is assumed that the number of cutting tips (n') is equal to the number of grains (n) on any section, the number of grains per unit area on any section can be evaluated as follows:

Consider a cuboidal element within the medium as shown in Fig. 3, having the width of the cuboide as equal to the diameter of the grain (d_g).

Then the volume of the cuboidal element (V) is given by,

$$V = A_2 \times d_g \tag{5}$$

where, A_2 is the surface area of the cuboidal element.

If the total number of grains in a cuboid is N, then number of grains per unit area (n) will be,

$$n = \frac{N}{A_2}. \tag{6}$$

Volume ratio (G) of the abrasive grains in the medium (cuboidal element) is defined as a ratio of the volume of the abrasive particles to the total volume of the cuboidal element.

Therefore,

$$G = \frac{N \times \frac{\pi d_g^3}{6}}{A_2 \times d_g},$$

$$\frac{N}{A_2} = n = \frac{6 \times G}{\pi \times d_g^2}. \tag{7}$$

Using Eq. 1 and Eq. 7,

$$h_t = \frac{d_g}{2nA_1} = \frac{d_g}{2 \times \frac{6 \times G}{\pi \times d_g^2} \times A_1} = \frac{\pi \times d_g^3}{12 \times G \times A_1}. \tag{8}$$

Thus, the total number of active grains (n_a) present in a cylindrical workpiece can be obtained as follows by using Eqs. 4 and 8.

$$n_a = \left[\frac{48 F_{am} G A_1}{\pi^2 \sigma d_g^4}\right]^{\frac{1}{2}} \tag{9}$$

As the total area of split cylindrical wokpiece is πDl, the active grains per unit area on the medium surface (n_1) are obtained as

$$n_1 = \frac{n_a}{\pi\ D\ l}. \tag{10}$$

A multivariable model is developed using available experimental data of active grains density. This model represents the active grains density in terms of extrusion pressure (P_e) and percentage abrasive concentration (C) as follows.

$$n_{mv} = 10.811 \times P_e^{0.628} \times C^{3.325} \tag{11}$$

Active grain density obtained from above theoretical model (Eq. 10) and multivariable regression model (Eq. 11) are compared with experimental results for the different experimental conditions (Fig. 11 and Fig. 12). The difference between the experimental and theoretical values seems to be due to the several assumptions made during the development of the model. In Fig. 12, active grain density is calculated by theoretical model only for 60% abrasive concentration. Theoretical active grain density for 50% and 55% abrasive concentration could not be calculated due to the insufficient measured axial force data available at these concentrations.

3 Prediction of radial forces

The force on a single grain in AFM should be known to model the AFM process mechanism of material removal. The depth of indentation of an abrasive grain into the workpiece material depends on the forces on it as discussed in reference [15]. The radial force acting on a single grain is responsible for its penetration into the workpiece and it can be estimated as,

$$F_{ng} = \sigma \times A$$

$$F_{ng} = \sigma \times \pi \times \left(\frac{b}{2}\right)^2 \quad (12)$$

where, A= projected area of contact between the workpiece material and abrasive grain, and b is the diameter of the projected area (Fig. 4).

Using Hertz theory [17], the depth of indentation d' of an abrasive grain in the workpiece during AFM can be estimated from Fig. 4,

$$d' = 1.550 \sqrt[3]{\frac{F_{ng}^2}{2RE_m^2}} \quad (13)$$

where, E_m=modulus of elasticity of workpiece material, N/mm^2.

4 Prediction of surface roughness

Using the force acting on a single grain (Eq. 12) and depth of indentation by a single grain (Eq. 13) as discussed in the preceding section, the material removal from the workpiece by each grain in each cycle can be evaluated. Then after, the surface roughness can be theoretically estimated as discussed in the following section.

The surface roughness model presented here is based on the following simplified assumptions:

1. It is considered that the diameter of all the grains is the same. Let the diameter of a representative grain be d_g (mm), then, from a given mesh size, it is estimated from the relation $d_g = {}^{28}/{M_e^{1.1}}$, where M_e is the mesh number [18].

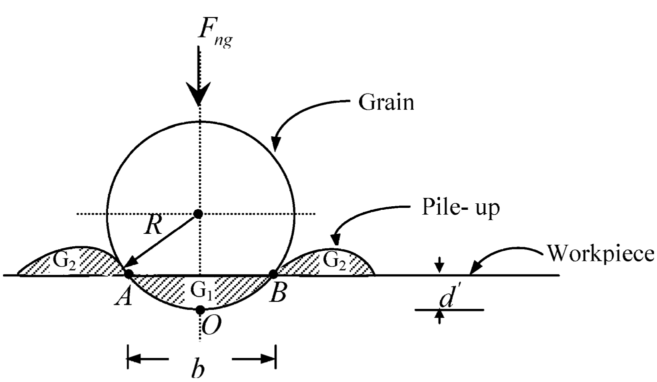

Fig. 4 Sphere indenting a plane surface elastically with side pile up material

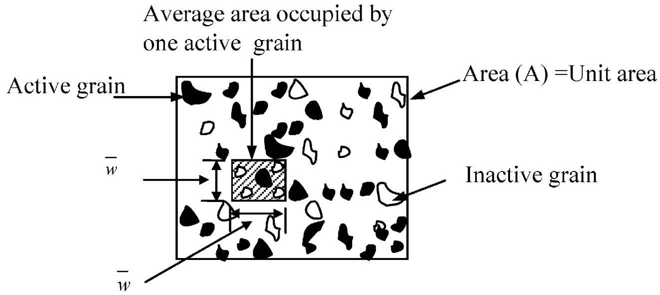

Fig. 5 A view of medium surface having active and inactive grains

2. The shape of an abrasive grain is approximated as a sphere, and not composed of acute cutting edges [19].
3. The path traced by an individual grain is a straight line, and there is no elastic deflection of grain into the medium.
4. During interaction between abrasive grain and workpiece, the material from the workpiece is displaced as a side pile-up. This assumption is supported by the scratching experiment [15] results.
5. The material from the peak of the profile is being removed in the form of side pile-up, and this piled up material gets filled on both sides in the valleys of the surface profile and results in deceptive improvement of surface roughness. In other words, material removal is assumed as 100 % plowing. However, in actual practice it may not be so.
6. All active abrasive grains are achieving the same depth of indentation.
7. The initial workpiece surface profile is considered as an equilateral triangular in shape. However, in actual practice they are non-uniform non-equilateral triangular in shape.

As the spherical grain (assumed rigid) moves over the surface of the workpiece, the grain penetrates to a depth (d'), the material in front of it gets deformed by shear and flows to the sides. For the case of pure plowing, no material is removed by chipping but it is only displaced to the side as shown in Fig. 4. In this case, it is assumed that G_2=0.5×G_1.

Fig. 6 Calculation of effective grain spacing

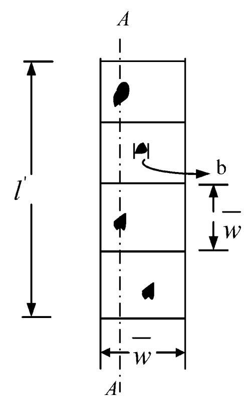

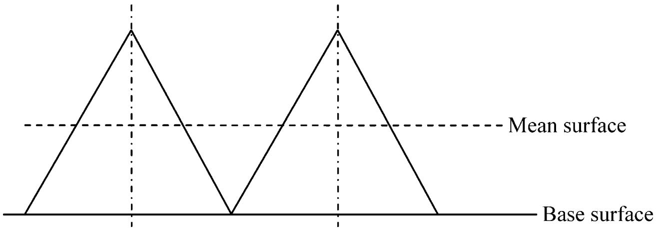

Fig. 7 Assumed initial surface topography of a workpiece

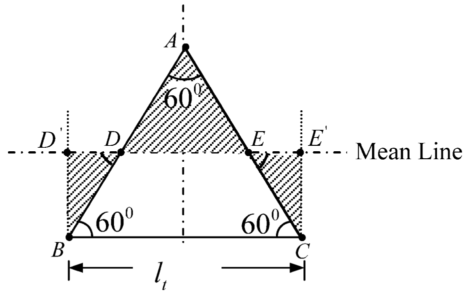

Fig. 9 Equilateral triangle

5 Effective grain spacing

It is assumed that all the grains are uniformly distributed and located at equal distances in all directions from its neighbors. Let a unit area on the medium surface has n_1 number of active grains which can be estimated by Eq. 10. Then, the average area occupied by one active grain will be $(1/n_1)$. If we assume that this area is a square shape then the side of the square (or mean spacing) $(\overline{w})$ between the grains is given by Eq. 14, Fig. 5 [13].

$$\overline{w} = (1/n_1)^{\frac{1}{2}} \tag{14}$$

Let us consider a strip of medium having width $\overline{w}$ and length l' (Fig. 6), passing over the workpiece surface. Suppose there are m number of active abrasive grains on this strip. Each abrasive grain will have a different diameter of indentation (=b) formed on the workpiece. However, to calculate an average grain spacing on this strip, the mean indentation diameter is taken as $\overline{b}$.

The probability of an arbitrary straight line A–A' (Fig. 6) to meet an abrasive grain (or edge) within this straight line (A–A') is $\overline{b}/\overline{w}$. If the grains are equally spaced, then the average grain spacing $(\overline{a})$ can be expressed by

$$\overline{a}=l'/\left(m \times \overline{b}/\overline{w}\right) \tag{15}$$

where, m is total number of cutting edges (or active grains) on the l' length of the strip of the medium.

Then, the number of active grains on this strip are given by

$$m = l'/\overline{w}. \tag{16}$$

If Eq. 16 is substituted in Eq. 15, then the average spacing between the grains is given by:

$$\overline{a} = \overline{w}^2/\overline{b}. \tag{17}$$

The length of the medium slug (l_m) passed in one stroke over the workpiece surface is evaluated from the volume constancy criterion as,

$$l_m = \frac{\pi r_{cy}^2 l_s}{\pi r_w^2} \tag{18}$$

where, r_{cy}=radius of medium cylinder, l_s=length of stroke, and r_w=radius of cylindrical workpiece.

The average number of grains (n_s) in one line over the total length of the medium slug,

$$n_s = \frac{l_m}{\overline{a}}. \tag{19}$$

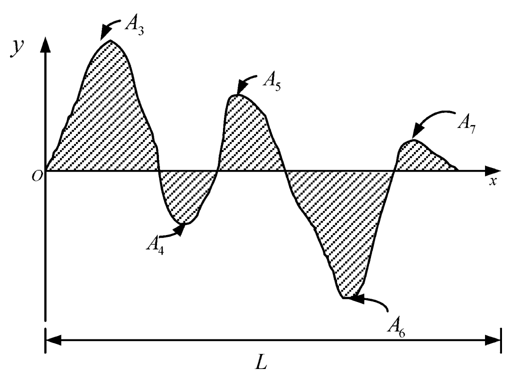

Fig. 8 Representation of methodology for evaluation of R_a value

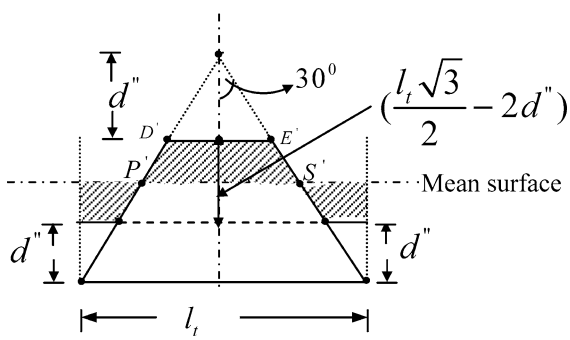

Fig. 10 Changing of mean surface

Table 1 Data used during theoretical analysis

Workpiece material	Mild steel
Flow pressure of workpiece material	304.1 N/mm^2 [22]
Modulus of elasticity of workpiece material	202086 N/mm^2 [22]
Density of silicon carbide abrasive	3220×10^{-9} kg/mm^3 [18]
Density of silly putty	1.14×10^{-6} kg/mm^3 [23]
Cylindrical workpiece dimensions	Diameter (D)=30 mm, Length (l)=47 mm.
Medium cylinder dimensions	Radius of medium cylinder (r_{cy})=43.5 mm
Average length of stroke	34.5 mm

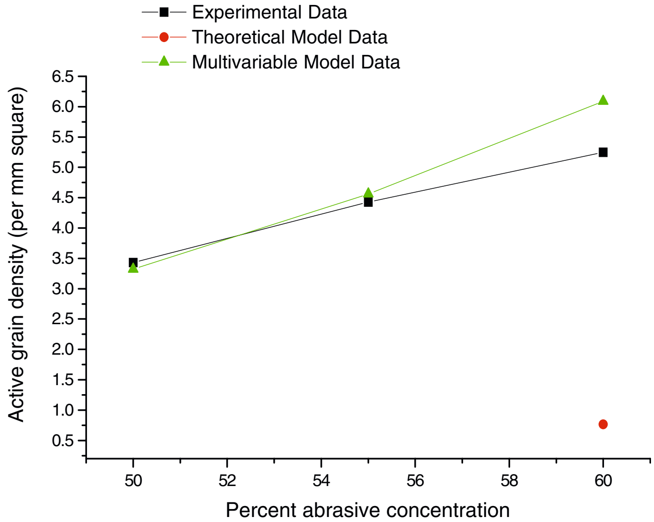

Fig. 12 Variation of active grain density with percent abrasive concentration. Experimental conditions: abrasive mesh size=80, extrusion pressure=6 MPa

6 Evaluation of R_a for the case of ploughing as the mode of material removal

It is assumed that the initial surface profile of workpiece consists of equilateral triangles (Fig. 7). The material removed by a single grain over a single equilateral triangle peak can be evaluated as follows.

Let us assume that in one stroke, n_s number of grains pass over one equilateral triangle peak, and each grain penetrates upto the depth equal to d'. Then the depth (d'') upto which the material is removed in one stroke over the triangular peak is given by

$$d'' = n_s \times d' \tag{20}$$

From Fig. 8, R_a can be defined as,

$$R_a = \frac{1}{L}\int_0^L |y|\, dx = \frac{A_3 + A_4 + A_5 + \ldots\ldots\ldots A_n}{L} \tag{21}$$

where, L is sampling length, and A_3, A_4,......, A_n are the areas.

Since we are assuming that the initial work surface profile is an equilateral triangle and one such triangle is

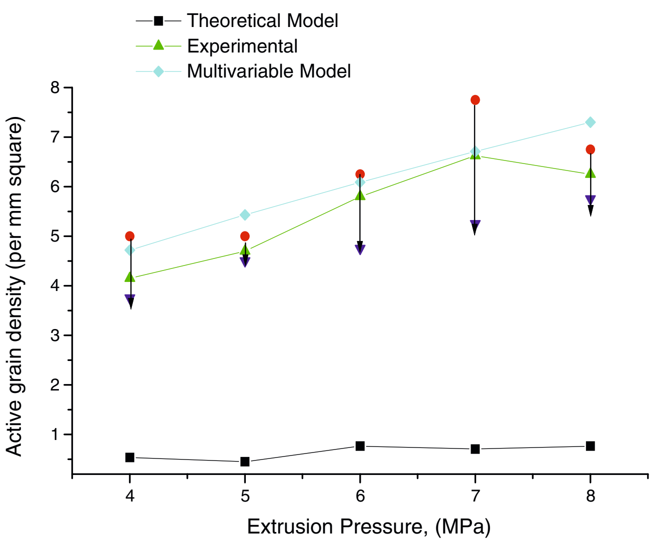

Fig. 11 Variation of active grain density with extrusion pressure. Experimental conditions: abrasive grain size=80; abrasive concentration=60%

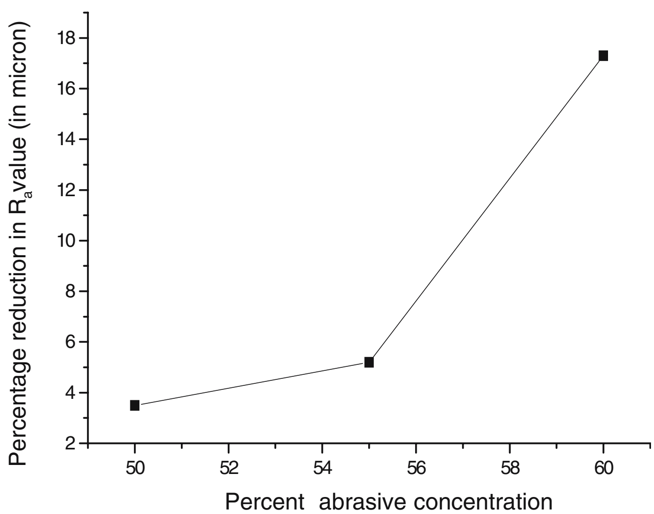

Fig. 13 Variation of percentage reduction in R_a with abrasive percent concentration. Experimental conditions: abrasive mesh size=80; extrusion pressure=6 MPa

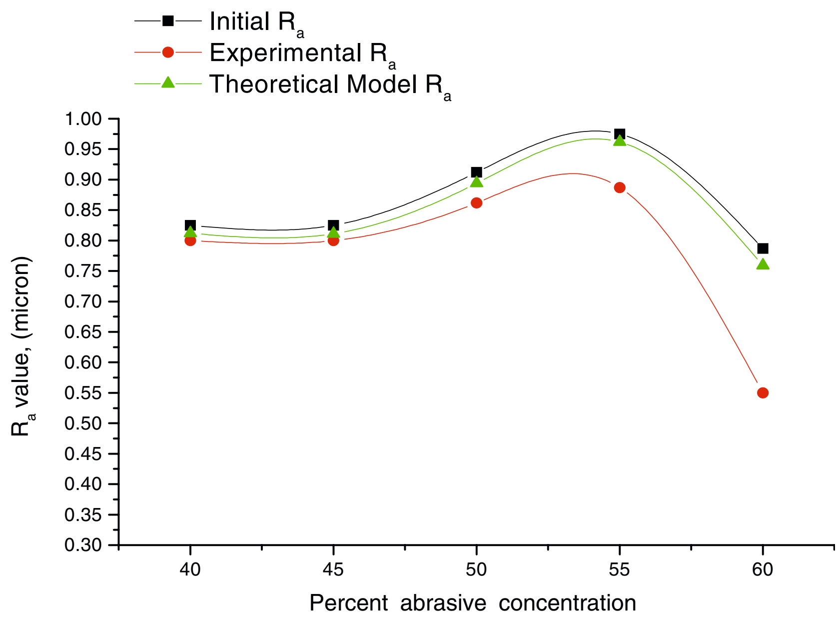

Fig. 14 Variation of surface roughness R_a value with percent abrasive concentration. Experimental conditions: abrasive mesh size=220; extrusion pressure=6 MPa

shown in Fig. 9. Let the base length of this equilateral triangle be l_t. If we consider the triangles $\Delta BDD'$ and $\Delta CEE'$ as the valleys and ΔDAE as the hill (peak) for a single triangle then the initial center line average (R_a) value of this equilateral triangular surface without any material removal from the peak can be estimated as,

$$= \frac{area\ of\ \Delta BDD' + area\ of\ \Delta DAE + area\ of\ \Delta CEE'}{l_t}$$

$$= R_a = \frac{l_t\sqrt{3}}{8}.$$

Hence,

$$l_t = \left(\frac{8\ R_a}{\sqrt{3}}\right). \tag{22}$$

It is assumed that the removed material is being filled equally on both sides in the nearest valleys to the same depth (d") or height as shown in Fig. 10. After one pass the

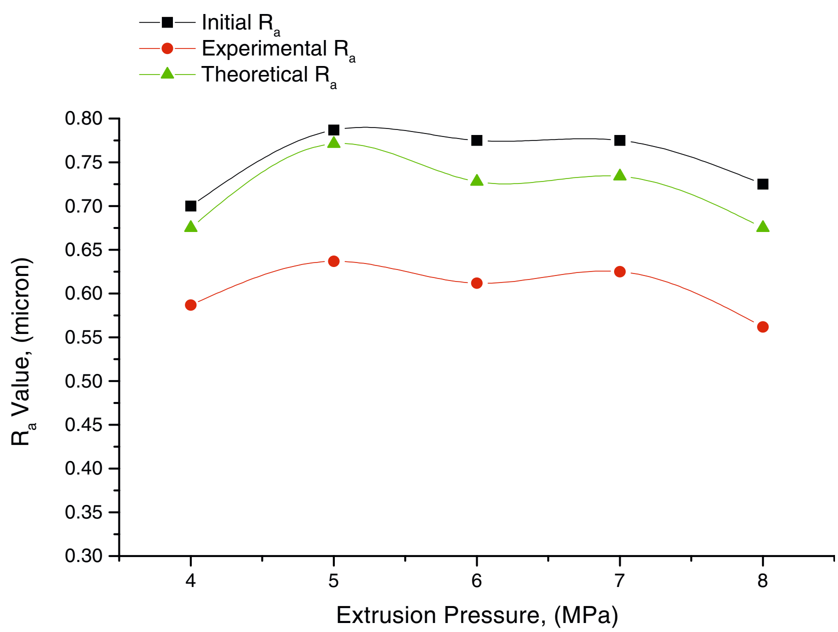

Fig. 15 Variation of surface roughness R_a value with extrusion pressure. Experimental conditions: abrasive grain size=80; abrasive concentration=60%

new surface becomes trapezium (Fig. 10). Its new surface roughness value (R_a) can be estimated as,

$$R_{a(new)} = \frac{2(area\ of\ trapezium\ D'E'S'P')}{l_t} = \frac{l_t\sqrt{3}}{8} - \frac{2\ d''^2}{l_t\sqrt{3}}. \quad (23)$$

Therefore, after completing *i* - number of passes the new R_a value can be estimated [21] as,

$$R_{a(new)} = \frac{l_t\sqrt{3}}{8} - \frac{2\,(i \times\ d'')^2}{l_t\sqrt{3}}. \quad (24)$$

Using the above analysis, the R_a value after *i* number of passes can be estimated for the case of equilateral triangular profile of the work surface.

7 Experimentation

Machining experiments are carried out on an AFM machine using mild steel as the workpiece material. The medium is a mixture of silly putty and silicon carbide abrasive particles. The experiments are conducted for various sets of process variables, i.e., extrusion pressure, abrasive mesh size, abrasive concentration, and initial workpiece roughness. For performing these experiments, compositions of two different abrasive mesh size (80 and 220) and different abrasive concentrations (40 to 60%) are prepared. The ranges for extrusion pressure and initial R_a value are chosen as 4 to 8 MPa and 0.7 to 0.9 µm, respectively. In these experiments, the effects of various process parameters on surface roughness (R_a) are studied. Average percent reduction in R_a value, over test duration (=22 number of cycles) are also estimated. Active grain density is measured for 80-mesh grain size. Data used for the theoretical analysis are listed in Table 1.

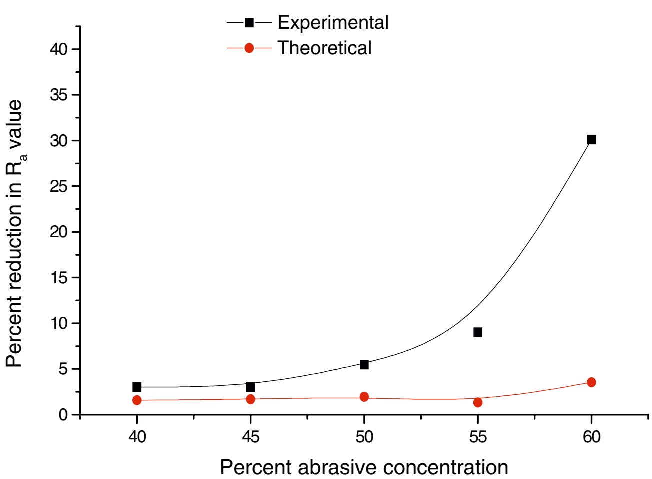

Fig. 16 Variation of percent reduction in R_a surface roughness with percent abrasive concentration. Experimental conditions: abrasive grain size=220; extrusion pressure=6 MPa

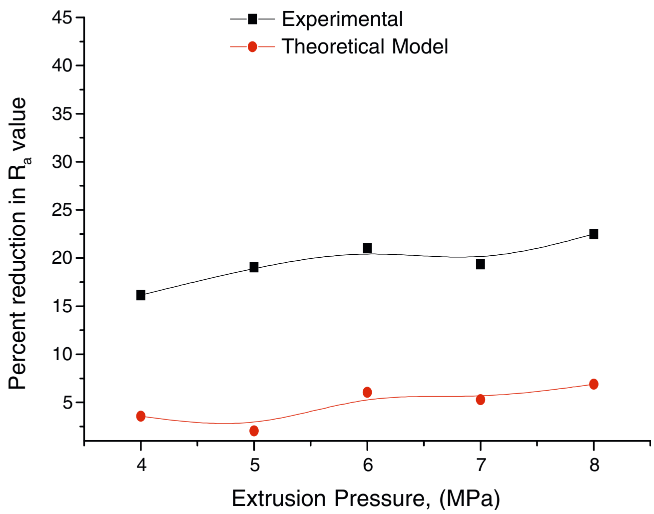

Fig. 17 Variation of percent reduction in R_a surface roughness with extrusion pressure, Experimental conditions: abrasive grain size=80; abrasive concentration=60%

8 Result and discussion

8.1 Active grain density

Experimental value of average active grain density is approximately directly proportional to the extrusion pressure up to 7 MPa extrusion pressure (Fig. 11) beyond which it starts declining. However, the theoretical value of active grain density is almost directly proportional to the extrusion pressure Fig. 11, and a similar trend is followed by multivariable model value (Eq. 11). Range (min. & max.) of the experimental data for active grain density is also plotted. In some cases, the variation in minimum and maximum values is high while in other cases it is low. These ranges show that there may be a chance of human error in counting the active grains in a unit area. It is also clear that both the models (theoretical and multivariable) are unable to capture the declining trend being exhibited by the experimental values. Secondly, the difference between the theoretical model values and experimental values is comparatively high.

Figure 12 shows that the active grain density (experimental, theoretical model, multivariable model) increases with increase in percent abrasive concentration. The experimental value is higher than the theoretical one. The values for other concentrations (except 60 %) could not be calculated using theoretical model due to the available insufficient experimental data.

9 Surface roughness R_a value

The percent reduction in R_a value is also increased with an increase in percent abrasive concentration (Fig. 13). It is so because the active grains density is also increasing with an increase in percent abrasive concentration (Fig. 12). The experimental results have been compared with the results computed using the theoretical model. Figures 14 and 15 show the variation in surface roughness with the change in percent abrasive concentration and extrusion pressure respectively. The variation pattern of experimental, and theoretical models in Figs. 14 and 15 are the same as variation pattern of initial R_a.

It is observed that with the increase in extrusion pressure and abrasive concentration a greater number of active grains (Figs. 11 and 12) come in contact with the workpiece. Therefore, in experiments and in theoretical model, the percentage reduction in R_a increases with increase in percent abrasive concentration and extrusion pressure (Figs. 16 and 17).

It is concluded in reference [15] that rubbing and plowing are the possible mechanisms of surface finish. On that basis we had assumed in theoretical model that due to plowing the valleys of the surface profile are being filled by material displaced from the peaks of the surface profile. This assumption seems to be valid when looking over the variation patterns of R_a in Figs. 14 and 15. Whatever is the initial R_a variation pattern before experiments the same is being followed by the final R_a achieved after experiments.

10 Conclusion

Based on the findings reported in this work, it is concluded that active grain density during the AFM process increases with an increase in extrusion pressure and percent abrasive concentration in the medium. This results in an increase in percent reduction in R_a value. Initial R_a of the workpiece is found to be an important parameter in AFM. Center line average R_a value after the AFM process can be predicted by considering the change in R_a value of an equilateral triangle as the initial surface profile of the workpiece.

Acknowledgement Authors acknowledge the financial support provided by the Department of Science and Technology, Government of India, New Delhi for the project entitled "Abrasive flow machining process" (Project no. III/5(2) 96ET). Authors are thankful to Mr. Pulak Mohan Pandey, Mechanical Engineering Department, I.I.T. Delhi for his help and suggestions in this work.

References

1. Rhoades LJ (1988) Abrasive flow machining. Manuf Eng:75–78
2. Williams RE, Rajurkar KP (1992) Stochastic modeling and analysis of abrasive flow machining. ASME J Eng Ind 114:74–81
3. Koshy P, Jain VK, Lal GK (1997) Stochastic simulation approach to modeling diamond wheel topography. Int J Mach Tools Manuf 37(6):751–761
4. Yoshikawa H, Sata T (1968) Simulated grinding process by Monte Carlo method. Ann CIRP 16:297–302
5. Law SS, Wu SM, Jogelkar AM (1973) On building models for the grinding process. Trans ASME J Eng Ind 95:983–991
6. Hamed MS, Whitehouse DJ, Buttery TC (1978) Random surface generation—integrated approach. Ann CIRP 27:499–504
7. Abrahamson EP II, Jahanmir S, Suh NP (1975) The effect of surface finish on the wear of sliding surfaces. Ann CIRP 24 (1):513–514
8. Jain RK, Jain VK (1999) Simulation of surface generated in abrasive flow machining process. Robot Comput-Integr Manuf 15:403–412
9. Pandey PM, Reddy NV, Dhande SG (2002) Improvement of surface finish by staircase machining in fused deposition modeling. J Mater Process Technol 132(1):323–331
10. Spurr RT (1976) The roughness of abraded metal surfaces. Wear 40:383–387
11. Dowson D, Whomes TL (1971) The effect of surface roughness upon the lubrication of rigid cylindrical rollers I Theoretical. Wear 18:129–140
12. Sakamoto T, Tsukizoe T (1977) Friction and prow formation in a scratch process of copper by a diamond cone. Wear 44:393–403
13. Tsuwa H (1964) An investigation of grinding wheel cutting edges. J Eng Ind Nov:371–382
14. Jain RK, Jain VK, Dixit PM (1999) Modeling of material removal and surface roughness in abrasive flow machining process. Int J Mach Tool Manuf 39:1903–1923
15. Gorana VK, Jain VK, Lal GK (2006) Force prediction during material deformation in abrasive flow machining. Wear 260 (1–2):128–139
16. Tanaka Y, Ikawa N (1966) Cutting mechanism of the bronze-bonded diamond wheel. Ann CIRP XIII:433–440
17. Lal GK, Brecker JN, Sauer WJ, Shaw MC (1970) Fifth annual report. Abrasive grain association investigation of abrasive grain characteristics. Carnegie Institute of Technology, Pittsburgh
18. Malkin S (1989) Grinding technology—Theory and application of machining with abrasives. Wiley, New York
19. Shaw MC (1971) A new theory of grinding. Proc Institution's Conference on Production Science in Industry, Melbourne, pp 73–78
20. Bowden FP, Moore AJW, Tabor D (1943) Ploughing and adhesion of sliding of the metals. J Appl Phys 14:80–91
21. Gorana VK (2006) Basic mechanics and parametric study of abrasive flow machining. Ph.D. Dissertation, Indian Institute of Technology Kanpur, KANPUR (U.P.) India
22. Design Data (1993) Faculty of Mech. Eng, PSG College of Technology, Coimbatore (INDIA)-641004
23. http://www.sillyputty.com